Modified-DBR-based semi-omnidirectional multilayer anti-reflection coating for tandem solar cells

Ali Bahrami†, Shahram Mohammadnejad, and Nima Jouyandeh Abkenar

Nanoptronics Research Center, Department of Electrical and Electronics Engineering, Iran University of Science and Technology, Tehran 16846-13114, *Iran*

(Received 17 March 2013; revised manuscript received 4 May 2013; published online 20 December 2013)

In this paper, multilayer antireflection coatings are designed by modifying the thickness of two and three paired layer distributed Bragg reflector (DBR) structure. Our proposed DBR-based structures show antireflection behaviors, in spite of the reflection treatment in traditional DBR structures. Firstly, the proposed structures are designed to be equivalent to the theoretical ideal triple-layer (TL) antireflection coating (ARC). Therefore, the problem of finding a suitable material for the middle layer of triple structure is solved. Simulation results show the significant equivalency for the reflectance of proposed structures to the ideal TL ARC at the same wavelengths and incident angles. Also, the design of the structure is changed in order to present the constant reflectance coefficient over a wide range of wavelengths. This structure enhances the omni-directionality of the multilayer ARC.

Keywords: antireflection coating, distributed bragg reflector, solar cell

PACS: 88.40.jm, 88.40.hj, 88.40.jp, 84.60.Jt **DOI:** 10.1088/1674-1056/23/2/028803

1. Introduction

The design of antireflection coatings (ARCs) is one of the most critical steps of solar cell development. The purpose of utilizing the ARC at the top of solar cells is to reduce the reflected photons from the cell surface. In tandem solar cells, a wide range of incident photons with different energy levels can be absorbed in the sub-cells of the tandem structure. So, it is important to guide as many incident photons as possible into the cell structure. TiO_2, Al_2O_3, ZnS, and MgF_2 are commonly used materials as the single and double layer ARCs.[1,2] These structures are only employed in single junction solar cells that work in a specific range of energy and they are not suitable for tandem structures. From the theoretical point of view, the combination of the mentioned materials can be utilized to design multilayer ARCs and solve this problem by reflecting the incident light in a wider range of wavelengths. However, the development of ARCs with more than two layers encounters some complexities. Especially in triple-layer (TL) ARCs, the refractive index of middle layer should be calculated by use of the upper and lower layer indices in order to present the ideal zero reflection. Nonetheless, it is hard to find a completely matched material with the theoretically achieved ideal refractive index for the middle layer. Therefore, it would be a great achievement if the characteristics of TL ARC could be obtained with a new equivalent two-material structure. For this purpose, we realize that the concept of reflection in distributed Bragg reflector (DBR) can be switched to antireflection by designing the structure layers with different thickness values. The designed structure can also enhance the omni-directionality behavior of the multilayer coating, which has been solved previously with the sophisticated structures such as nanostructures or graded refractive index ARCs.[3,4]

In this paper, we modify the thickness values of layers in two and three paired layer DBRs made from two commonly used materials and propose a new structure as the antireflection coating. The simulation results of the structures show the same reflection characteristics as those of the TL ARC over different ranges of wavelengths and incident angles. Also, the modified-DBR structure is redesigned in order to show the constant reflection in a wavelength range of lower than 1000 nm. The three-pair structure presents the semi-omnidirectional behavior in the mentioned wavelengths. The next section of this paper describes the design characteristics and the theoretical calculations of the multilayer structures by utilizing the transfer matrix method. In Section 3, the simulation results of the DBR-based equivalent structure for TL ARC along with smoothed reflectance structures will be presented. The paper will end with the discussion and conclusion.

2. Design

For zero reflectance calculations in multilayer structures, the thickness of each layer in the design wavelength, λ_D, is related to the refractive index, as follows:[5]

$$\text{layer thickness} = \frac{\lambda_D}{4 \times \text{refractiveindex}}. \quad (1)$$

The amplitude relation of the electromagnetic fields in the interface of layers in N-layer structure can be deduced from

†Corresponding author. E-mail: abahrami@iust.ac.ir

© 2014 Chinese Physical Society and IOP Publishing Ltd

transfer matrix method, as follows:[6]

$$M_{\rm eq}=\prod_{j=1}^{N}\begin{bmatrix}\cos\varphi_j & \left(\dfrac{\rm i}{n_j^{\rm eff}}\right)\sin\varphi_j\\ {\rm i}n_j^{\rm eff}\sin\varphi_j & \cos\varphi_j\end{bmatrix}\equiv\begin{bmatrix}m_{11} & m_{12}\\ m_{21} & m_{22}\end{bmatrix}, \quad (2)$$

where n_j, $\varphi_j=2\pi n_j^{\rm eff}d_j/\lambda_{\rm in}$, and d_j are the refractive index, phase thickness, and layer thickness of the j-th layer, respectively, with $\lambda_{\rm in}$ being the incident wavelength, and $n_j^{\rm eff}$ the effective refractive index equal to $n_j^{\rm eff}=n_j\cos\theta_j$ for the parallel polarization and $n_j^{\rm eff}=n_j/\cos\theta_j$ for the normal polarization with θ_j as the incident angle of the j-th layer; the parameters m_{kl} for k,l =1,2 are the elements of matrix $M_{\rm eq}$. The reflection coefficient of the N-layer structure with equal matrix of $M_{\rm eq}$ can be calculated as follows:

$$r=\frac{\gamma_0 m_{11}+\gamma_0\gamma_{\rm s}m_{12}-m_{21}-\gamma_{\rm s}m_{22}}{\gamma_0 m_{11}+\gamma_0\gamma_{\rm s}m_{12}+m_{21}+\gamma_{\rm s}m_{22}}, \quad (3)$$

where $\gamma_0=\sqrt{\mu_0\varepsilon_0}\cos\theta_0$; $\gamma_{\rm s}=n_{\rm s}\sqrt{\mu_0\varepsilon_0}\cos\theta_{\rm s}$; μ_0 and ε_0 are the vacuum permeability and permittivity respectively.

A TL structure is shown in Fig. 1(a). The refractive index of middle layer, $n_{\rm m}$, in the TL ARC is the geometric mean of upper and lower layer indices.

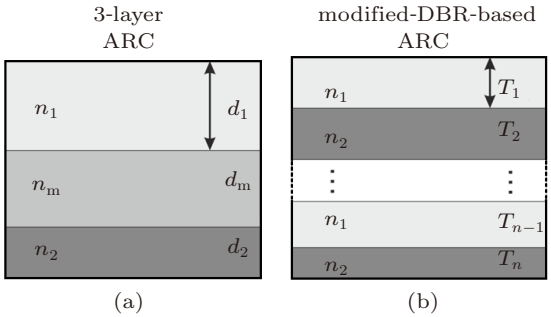


Fig. 1. Schematics of (a) TL ARC structure and (b) multilayer modified-DBR-based ARC structure.

According to Eq. (1), for zero reflectance in an ideal TL structure in the case of normal incidence, n_jd_j will be equal for all of the designed layers. Therefore, in the normal incidence ideal zero reflectance TL structure for design wavelength of 650 nm,

$$\varphi_1=\varphi_2=\varphi_3=\varphi=\frac{0.325\pi}{\lambda_{\rm in}} \quad (4)$$

and the reflectance coefficient can be achieved as follows:

$$r_{3L}=\frac{\begin{array}{l}+{\rm i}\left(\dfrac{n_1n_2}{n_{\rm m}}-\dfrac{n_{\rm s}n_{\rm m}}{n_1n_2}\right)\sin^3\varphi+\left(-\dfrac{n_2}{n_{\rm m}}-\dfrac{n_{\rm m}}{n_1}-\dfrac{n_2}{n_1}+\dfrac{n_1n_{\rm s}}{n_2}+\dfrac{n_1n_{\rm s}}{n_{\rm m}}\dfrac{n_{\rm m}n_{\rm s}}{n_2}\right)\sin^2\varphi\cos\varphi\\ +{\rm i}\left(\dfrac{n_{\rm s}}{n_2}+\dfrac{n_{\rm s}}{n_{\rm m}}+\dfrac{n_{\rm s}}{n_1}-n_1-n_{\rm m}-n_2\right)\sin\varphi\cos^2\varphi+(1-n_{\rm s})\cos^3\varphi\end{array}}{\begin{array}{l}-{\rm i}\left(\dfrac{n_1n_2}{n_{\rm m}}+\dfrac{n_{\rm s}n_{\rm m}}{n_1n_2}\right)\sin^3\varphi+\left(-\dfrac{n_2}{n_{\rm m}}-\dfrac{n_{\rm m}}{n_1}-\dfrac{n_2}{n_1}-\dfrac{n_1n_{\rm s}}{n_2}-\dfrac{n_1n_{\rm s}}{n_{\rm m}}-\dfrac{n_{\rm m}n_{\rm s}}{n_2}\right)\sin^2\varphi\cos\varphi\\ +{\rm i}\left(\dfrac{n_{\rm s}}{n_2}+\dfrac{n_{\rm s}}{n_{\rm m}}+\dfrac{n_{\rm s}}{n_1}+n_1+n_{\rm m}+n_2\right)\sin\varphi\cos^2\varphi+(1+n_{\rm s})\cos^3\varphi\end{array}}. \quad (5)$$

The TL structure can be substituted with an alternative structure of two-material combination and by making DBR-based structures with different thickness values. The modified-DBR-based ARC structure is presented in Fig. 1(b). By utilizing Eq. (2), the layer thickness values of proposed structure will be chosen in order to reach a reflection behavior similar to that the TL ARC possesses. Also, the same structures with different thickness values can be designed for presenting a constant reflectance over a wide range of wavelengths.

3. Simulation results

In this section, the thickness values of layers in DBR structure are modified with the optimization algorithms[7] in order to achieve two different purposes; that is,

1) Making modified-DBR-based ARC used as an equivalent structure for optimum TL ARC; and,

2) Introducing semi-omnidirectional modified-DBR-based ARC with smoothed reflection curve.

The simulation results of the structures with the mentioned purposes are described as follows.

3.1. Equivalent structure for optimum TL ARC

$MgF_2(1.39)/TiO_2(2.44)$ combination is the most commonly used structure for double-layer ARC. The TL structure can be designed by finding a suitable material for use as the middle layer between MgF_2 and TiO_2. The zero reflectance theoretical calculations show that the optimum refractive index for the middle layer of the mentioned TL ARC is 1.84. However, an available matched material corresponding to this refractive index could not be found. Nevertheless, we assume the 1.39/1.84/2.44 to be the refractive indices of optimum structure for TL ARC in the next considerations. The initial design for calculating the optimum thickness of TL ARC is accomplished for a wavelength of 650 nm that corresponds to the peak point of solar spectral energy. In order to avoid the problem of choosing the suitable material for theoretically designed TL structure, in this paper we propose a two-material DBR-based structure that can be employed instead of three-material TL ARC.

The layers are designed in order to obtain proper values for sets of $T_1/T_2/T_3/T_4$ and $T_1/T_2/T_3/T_4/T_5/T_6$ for triple equivalent quadruple layer (TEQL) and senary layer (TESL) structures. These structures should present the same reflectance values as the TL ARC in different ranges of wavelengths and incident angles. The simulation results show a good coincidence with TL ARC for TESL in comparison with TEQL. Figure 2 shows the comparison of reflectance curves among three-material TL ARC, the modified-DBR-based TEQL, and TESL antireflection structures in the case of normal incidence.

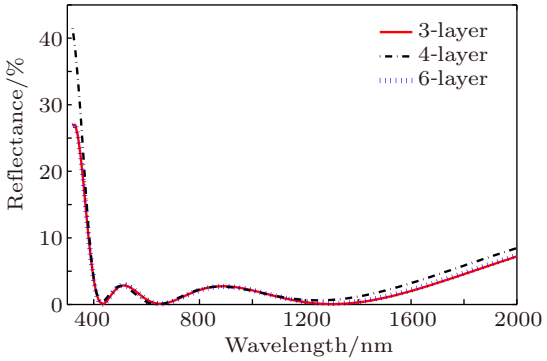


Fig. 2. (color online) Spectral reflectance curves of optimum TL and modified-DBR-based TEQL and TESL ARC.

As can be seen in Fig. 2, the coincidence of TEQL and TESL structures with TL ARC starts from the wavelengths of 320 nm to more than 2000 nm. The most important assumption considered during the process of finding the best thicknesses is that the total thickness of proposed structure should be comparable to that of the optimum TL ARC. By comparing the reflection curves in Fig. 2 for TEQL and TESL, it can be deduced that the matching of the structure with TL ARC is enhanced with the increasing number of layers. It should be noted that the process of finding appropriate thickness values for higher number of layers will be considerably time consuming. However, it is obvious that the TESL designed structure is perfectly matched with TL ARC and that a further increase of the layers will be ineffectual. The obtained sets of thickness values for TEQL and TESL ARCs are 120/22/31/84 and 117/9/25/17/25/76, respectively.

In addition, the TEQL and TESL structures should have the same behaviors as TL ARC at different incident angles. Our simulation results show these perfect matchings over the different incident angles. Figure 3 illustrates the dependences of the reflectance on the incident angle for the wavelengths of 400, 650, and 900 nm.

Figure 3 shows that the TEQL and TESL ARCs with the proper thickness values can reflect the same energy of photons as the ideal TL ARC. It should be noticed that the total thickness of both structures is less than 272-nm thickness of ideal TL ARC. Therefore, it can be understood that the proposed structure solves the problem of finding an unknown material matched with calculated ideal refractive index just by using two commonly used materials with a lower overall thickness.

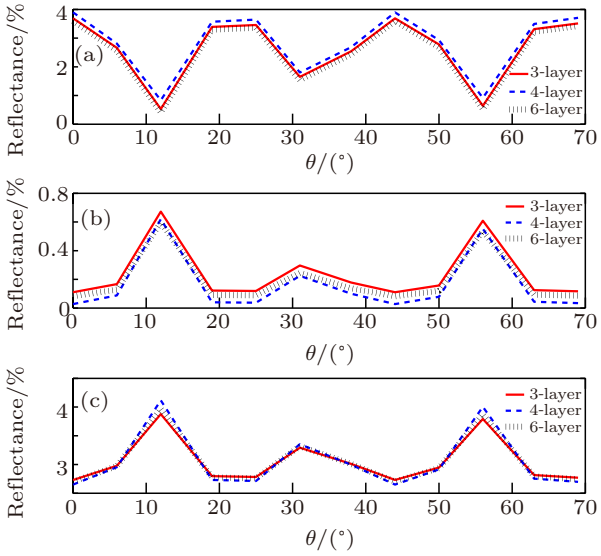


Fig. 3. (color online) Dependences of reflectance on the incident angle for the wavelengths of (a) $\lambda = 400$ nm, (b) $\lambda = 650$ nm, and (c) $\lambda = 900$ nm.

3.2. Constant reflectance

The proposed structure of the ARC can be redesigned in order to present a low and constant reflectance coefficient which can be used as a broadband ARC in tandem solar cells. The reflectance curves of the new structures are shown in Fig. 4. The 80/6/14/56 and 92/10/3/3/13/48 set of thickness values have been achieved for 4- and 6-layer structures as the smoothed reflectance quadruple layer (SRQL) and senary layer (SRSL) ARCs, respectively.

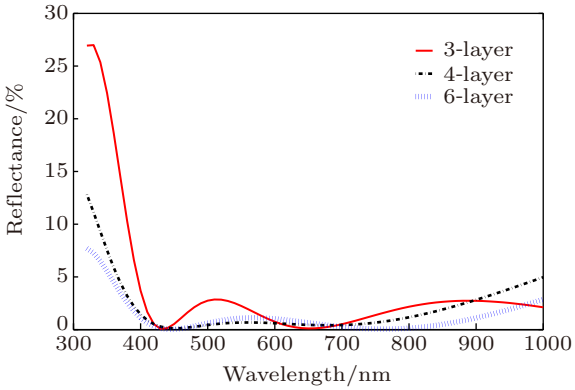


Fig. 4. (color online) Reflectance curves of TL and DBR-based structures designed for achieving the constant reflection.

A comparison of reflection coefficient between SRQL and SRSL ARC shows that the later one presents an almost constant reflection in a wider range of wavelengths. It can be seen that the reflectance of SRSL is lower than 1% for a wavelength range of 500 nm. These structures have been designed for a normal incidence. It should be noted that the structures with higher number of layers can just slightly improve the reflection characteristics. The dependences of the reflectance on the incident angle for different wavelengths are presented in Fig. 5.

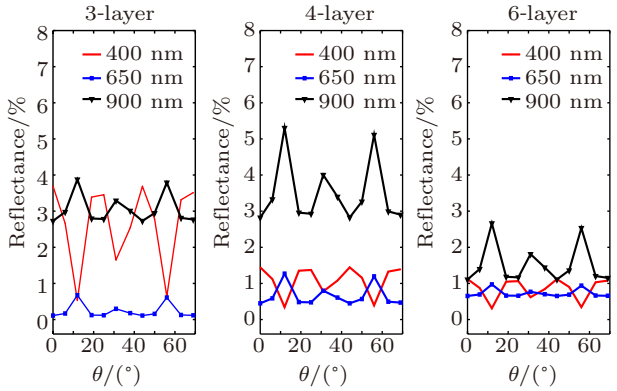


Fig. 5. (color online) Curves of reflectance versus incident angle for TL, SRQL, and SRSL ARCs at different wavelengths.

As can be seen in Fig. 5, the SRSL ARC demonstrates a lower reflectivity in comparison with TL and SRQL ARCs at different wavelengths. Indeed, the TL ARC that has been designed for a specific wavelength of 650 nm is not applicable for other wavelengths. Also, the SRQL structure can reduce the value of reflectivity in a small range of wavelengths. However, the SRSL presents the lower reflectance over a wider range of wavelengths. This concept can also be deduced from Fig. 4. Also, the SRSL structure shows the lower reflectivity variations for a specific wavelength over a wide range of incident angles. So, from this point of view, better omnidirectionality can be achieved by increasing the number of layers.

4. Discussion

The multilayer ARCs with the broadband antireflective behavior can be utilized in tandem solar cells. In this paper, the designed ARCs are employed at the top of the AlGaAs/GaAs solar cell which is shown in Fig. 6.

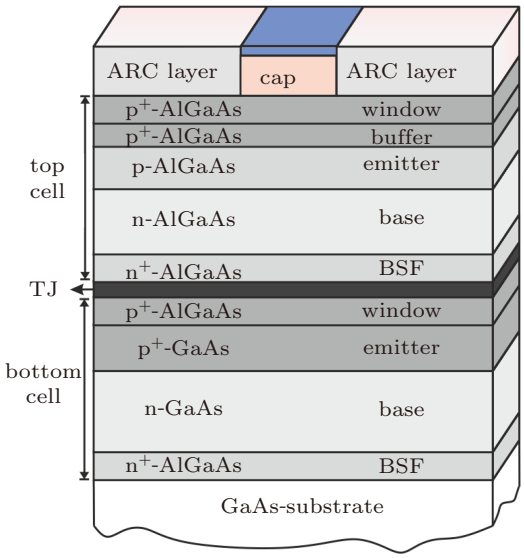


Fig. 6. (color online) Structure of AlGaAs/GaAs tandem solar cell.

The simulation results obtained by utilizing the TL, TEQL, TESL, SRQL, and SRSL structures as the antireflection coating of AlGaAs/GaAs solar cell, that is, the power conversion efficiency, fill factor, short circuit current, and open circuit voltage in 1sun AM1.5G are presented in Table 1.

Table 1. Simulation results of the tandem solar cell with utilizing the proposed ARCs.

ARC	η/%	FF/%	I_{SC}/(mA/cm^2)	V_{OC}/V
TL	23.39	91.24	11.05	2.32
TEQL	23.374	91.23	11.045	2.32
TESL	23.4	91.24	11.052	2.32
SRQL	23.5	91.26	11.1	2.32
SRSL	23.7	91.24	11.2	2.32

As mentioned above, the TEQL and TESL structures are designed in order to show the same reflectance characteristics as the TL ARC. Simulation results of tandem solar cell for TEQL and TESL shown in Table 1 emphasize that the theoretical zero reflection TL ARC can be replaced with the mentioned designed structures. Also, it is obvious that the TESL ARC shows more coincidences with the TL structure than with the TEQL. Consequently, the TESL structure shows the reflection coefficients equal to those the TL ARC does at different wavelengths and incident angles and can be completely used instead of TL ARC. In addition, as shown in Fig. 4, the SRQL and SRSL structures are designed in order to present a constant reflection coefficient lower than that of the TL ARC. Therefore, the mentioned structures should present the optimized results in comparison with the previously discussed ARCs. Table 1 emphasizes that the SRQL and SRSL structures can produce higher short circuit currents and efficiencies than the other ARCs. The current–voltage (I–V) curves of tandem solar cell are compared with those of the designed ARCs in Fig. 7.

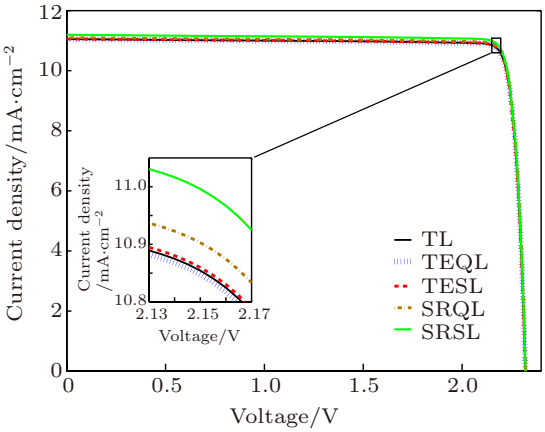


Fig. 7. (color online) The I–V curves of tandem solar cell with different types of ARCs.

As can be seen in Fig. 7, the highest short circuit current of AlGaAs/GaAs tandem solar cell can be obtained in the case of SRSL ARC. According to the high coincidences of TEQL and TESL structures with TL ARC, the partial projections of I–V curve are presented in the inset of Fig. 7.

5. Conclusion

We propose different DBR-based ARCs by modifying the thickness values of constructive layers. The problem of finding suitable materials in theoretical ideal triple layer ARCs is solved by designing two- and three-pair DBR-based structures. Our simulation results show that six-layer structure could present more coincidences with TL ARC than four-layer structure. The design of the structures is changed in order to present the constant reflectance coefficient over a wide range of the wavelengths. The designed structures are utilized as ARC in an AlGaAs/GaAs tandem solar cell. Based on simulation results, the smoothed reflectance six-layer ARC shows further performance enhancement in comparison with the other structures.

References

[1] Jung S M, Kim Y H, Kim S I and Yoo S I 2011 *Curr. Appl. Phys.* **11** 538

[2] Bahrami A, Mohammadnejad S and Soleimaninezhad S 2013 *Opt. Quantum Electron.* **45** 161

[3] Diedenhofen S L, Grzela G, Haverkamp E, Bauhuis G, Schermer J and Rivas J G 2012 *Sol. Energy Mater. Sol. Cells* **101** 308

[4] Tommila J, Polojarvi V, Aho A, Tukiainen A, Viheriala J, Salmi J, Schramm A, Kontio J M, Turtiainen A, Niemi T and Guina M 2010 *Sol. Energy Mater. Sol. Cells* **94** 1845

[5] Macleod H A 2001 *Thin-Film Optical Filters* (London: IOP)

[6] Bouhafs D, Moussi A, Chikouche A and Ruiz J M 1998 *Sol. Energy Mater. Sol. Cells* **52** 79

[7] Mansouri T, Farasat A, Menhaj A B and Moghadam M R S 2011 *Expert. Syst. Appl.* **38** 4866